



Boundary exchange completes the marine Pb cycle jigsaw

Mengli Chen^{a,1} , Gonzalo Carrasco^b, Ning Zhao^{c,1} , Xianfeng Wang^{b,d} , Jen Nie Lee^e , Jani T. I. Tanzil^a, Kogila Vani Annammala^f , Seng Chee Poh^e , Federico M. Lauro^{d,g} , Alan D. Ziegler^h , Decha Duangnamonⁱ, and Edward A. Boyleⁱ

Edited by Donald Canfield, Syddansk Universitet, Odense M., Denmark; received August 10, 2022; accepted January 5, 2023

Material fluxes at the land–ocean interface impact seawater composition and global cycling of elements. However, most attention has been focused on the fluvial dissolved fluxes. For elements like lead (Pb), whose fluvial particulate flux into the ocean is two orders of magnitude higher than the dissolved counterpart, the role of particulates in elemental cycling is potentially important but currently less appreciated. Using both chemical analyses on samples collected from around equatorial Southeast Asia and model simulations, we show that particulate–dissolved exchange is an important mechanism controlling the concentration and isotopic composition of dissolved Pb in the ocean. Our model indicates that Pb contributed from particulate–dissolved exchange at ocean boundaries is larger than, or at least comparable to, other major Pb sources to the seawater before the Anthropocene, when the anthropogenic Pb was absent. Our work highlights the importance of boundary exchange in understanding marine element cycling and weathering–climate feedback.

marine elemental cycling | isotope | Southeast Asia | boundary exchange | Pb

The transfer of materials from land to ocean impacts the chemical composition of seawater and the cycling of elements in the coupled ocean–atmosphere–lithosphere system (1, 2). When assessing marine elemental cycling, the land–ocean material exchange has traditionally been considered mainly through dissolution of terrestrial-sourced aerosols (3) and the fluvial transport of dissolved elements, together with other oceanic sources such as hydrothermal emanations and deep-sea sediments that release some elements in dissolved form (4). Contributions from fluvial particles remain poorly investigated for most of the elements (1). However, as revealed by increasing evidence (5–7), fluvial particles may hold the key to understanding the missing pieces in the “jigsaw” of elemental cycling in the global ocean.

Lead (Pb) is an element of interest in this issue because the global land-to-ocean particulate flux of Pb is several hundred times higher than the dissolved flux (2, 8, 9). As such, the contribution of Pb from fluvial particulates is potentially an important part of the natural cycling of Pb. The global sink of Pb in the oceans involves transfer of dissolved Pb to the deep ocean sediment, which is estimated as 6.3×10^7 mol/y based on the sediments across the Atlantic and Pacific (10). The major known natural sources of marine Pb include dissolution of aeolian dust [$\sim 7.70 \times 10^6$ mol/y (11, 12)]; volcanic aerosols [$\sim 6.76 \times 10^6$ mol/y (11)]; as well as hydrothermal activity [$\sim 1.95 \times 10^7$ mol/y (13, 14)]. Collectively, these sources constitute only a fraction of the marine Pb sink, leaving an enormous imbalance of $\sim 2.9 \times 10^7$ mol/y, a large portion of which could potentially be derived from fluvial sources. The total fluvial dissolved Pb flux today ($\sim 1.16 \times 10^7$ mol/y) (15), which is overprinted with likely a large contribution of anthropogenic Pb (16), is too low to balance the natural Pb cycling in the ocean. Removing the anthropogenic contribution would render an even smaller natural fluvial dissolved flux to this imbalance. Missing in the calculation of marine lead budget is the contribution of Pb derived from fluvial particulates entering the marine environment from land masses, followed by release into the dissolved form. The current imbalance suggests this contribution could be substantial, on the order of at least $\sim 1.74 \times 10^7$ mol/y, and differing for contemporary versus historical times before anthropogenic Pb was prevalent.

Multiple lines of evidence [e.g., radioactive ^{210}Pb (17–19), budget estimations (2, 8, 9), direct measurements (20)] suggest that the transport of fluvial particulate Pb is about two orders of magnitude larger than the dissolved counterpart; therefore, the dissolution of even a small fraction of particulate Pb into seawater could greatly impact marine Pb cycling (cf. 10). Exchanges at ocean–land boundaries have been shown to be important mechanisms in the cycling of several elements including neodymium, strontium, and silica (1, 21, 22). Similarly, the exchange of Pb between dissolved and particulate phases has been revealed in several recent studies around the world, including the western Philippine Sea (23), Celtic Sea (24), and Eastern Atlantic margin (25). Additionally, a closed-system experiment using water from the Johor River estuary (equatorial Southeast Asia)

Significance

Exchange of chemical species and matter at ocean boundaries influences the composition of seawater and is an important process affecting biogeochemical element cycling involving interactions between the atmosphere, hydrosphere, geosphere, and biosphere. However, systematic quantification on the processes and budgets remains scarce. Here, through field, laboratory analysis and modeling, we show that the adsorption–desorption exchange of lead (Pb) between the particulate and dissolved pools at ocean boundaries accounts for about 30 to 40% of Pb input into the ocean before the Anthropocene, which finally resolves the paradox of imbalanced natural sources and sinks of Pb in the ocean. With Pb as an example, our study adds a crucial piece of evidence to the importance of boundary exchange in marine element cycling.

Author contributions: M.C., G.C., N.Z., and E.A.B. designed research; M.C., G.C., J.N.L., and K.V.A. performed research; M.C., G.C., X.W., J.T.I.T., S.C.P., F.M.L., and D.D. contributed new reagents/analytic tools; M.C. and N.Z. analyzed data; M.C., G.C., and X.W. provided resources for part of the project; J.N.L., K.V.A., S.C.P., A.D.Z., and D.D. provided sampling permits and conducted fieldwork; J.T.I.T. contributed sampling permits, provided resources for part of the project; F.M.L. provided resources for part of the fieldwork; E.A.B. provide supervision and resources for part of the project; and M.C., N.Z., and A.D.Z. wrote the paper.

The authors declare no competing interest.

This article is a PNAS Direct Submission.

Copyright © 2023 the Author(s). Published by PNAS. This article is distributed under [Creative Commons Attribution-NonCommercial-NoDerivatives License 4.0 \(CC BY-NC-ND\)](https://creativecommons.org/licenses/by-nc-nd/4.0/).

¹To whom correspondence may be addressed. Email: mengli.chen@nus.edu.sg or nzhao@sklec.ecnu.edu.cn.

This article contains supporting information online at <https://www.pnas.org/lookup/suppl/doi:10.1073/pnas.2213163120/-DCSupplemental>.

Published January 30, 2023.

directly showed fast and reversible particulate-dissolved exchange of Pb (26). While these studies indicate that exchanges of Pb between dissolved and particulate phases occur at ocean boundaries, the underlying mechanisms and geographical extent remain unexplored. Also unknown is the contribution of this exchange in the cycling of Pb in the global ocean.

The southern and eastern part of Asia are highly relevant for particulate-dissolved exchanges of elements because this area accounts for about two-thirds of the global fluvial sediment flux into the ocean (27) (Fig. 1A). Although rivers in this region are shorter than many continental rivers elsewhere, they have disproportionately high-particulate discharges due to high erosion rates associated with steep topographic relief and climates featuring periods of heavy rainfall (1, 27). In this study, through chemical

analysis and model simulations, we trace the dynamics of particulate-dissolved exchange and estimate its contribution to dissolved Pb concentration and isotopic composition in the waters surrounding the Malayan Peninsula in equatorial Southeast Asia. Further, we assess the contribution of particulate-dissolved exchange on the global scale for the present-day and pre-Anthropocene ocean.

Results

Geographical Distribution of Seawater Pb Concentration and Pb Isotopes. From fieldwork, we found that the dissolved Pb concentration in the seawater around the Malayan Peninsula ranged from 24 to 368 pmol/kg (Fig. 2). We treated one unusually high concentration value (1,989 pmol/kg; Johor River Stn 7)

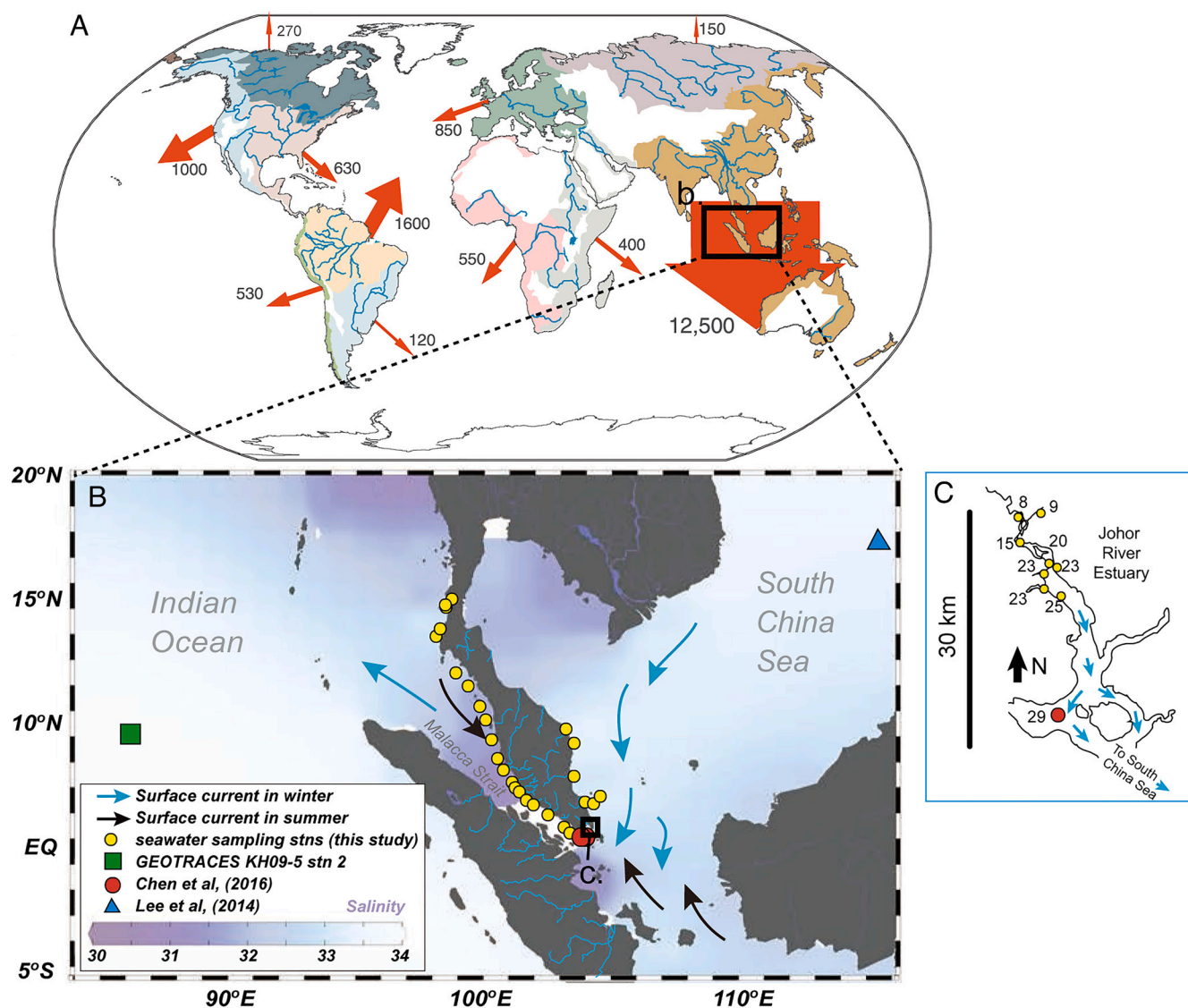


Fig. 1. (A) Fluvial discharge of sediments to the global ocean replotted from ref. 27. Numbers are mean annual suspended sediment discharges (million tons/year). Colour shades represent the illustrative catchment regions with major rivers highlighted. (B) The seawater sampling stations in this study (yellow circles) and seawater stations in the literature are shown for comparison [red circles, green rectangle, blue triangle (26, 28, 29)]. The rivers relevant to the sampling sites are highlighted in blue. The surface ocean currents are marked with arrows. (C) Sampling stations in the Johor River estuary with salinity values (pss) marked next to the station locations; the estuary is highlighted with a square in panel B.

as an outlier that probably resulted from particulate leakage during filtration, as its isotope composition is consistent with other samples (Fig. 3). Stations with elevated Pb concentrations (>100 pmol/kg) are generally located near major cities (Fig. 2A), which have a high prevalence of Pb sources associated with anthropogenic activities. In contrast, Pb isotopes in the dissolved pool of seawater displayed a different geographical distribution: Waters with high $^{206}\text{Pb}/^{207}\text{Pb}$ ratios were generally found near river mouths (Fig. 2B), irrespective of inputs from upstream or downstream cities. The difference between the distributions of Pb concentration and isotopic composition indicates separate or nonuniform controls on the two variables.

Source Apportionment of Seawater Pb Isotopes. The linear relationship between Pb isotope ratios of seawater in the triple isotope space signifies the existence of two primary endmembers (Fig. 3A), one being regional aerosols. Present-day Southeast Asian/Indian aerosols' isotope signatures range from 1.12 to 1.15 for $^{206}\text{Pb}/^{207}\text{Pb}$ (31–33), overlapping with the Pb signature in the

seawater of the southern South China Sea and Eastern Indian Ocean (28, 29). The Pb isotopic composition of regional aerosols also overlaps with two seawaters in our study sampled from the most oceanic sites (Ranong, Thailand, flushed by Andaman Sea water), lending evidence that aerosol Pb is an endmember for seawater (Fig. 3B). The second endmember could be either fluvial-transported anthropogenic Pb or crustal Pb. However, the geographical differences between seawater Pb concentration and Pb isotopic compositions provides evidence against fluvial anthropogenic Pb being an endmember (Fig. 2). Therefore, crustal Pb is likely the other endmember. The isotopic compositions of crustal Pb and regional aerosol Pb bracket almost all the seawater samples examined (Fig. 3A). A crustal Pb endmember also reasonably explains the geographical distribution of Pb isotopes, as enrichment of crustal Pb with high $^{206}\text{Pb}/^{207}\text{Pb}$ values is expected at river mouths where fluvial export to the ocean is the highest.

We also found that estuarine Pb isotope ratios vs salinity do not follow a conservative mixing line (Fig. 3C), showing higher

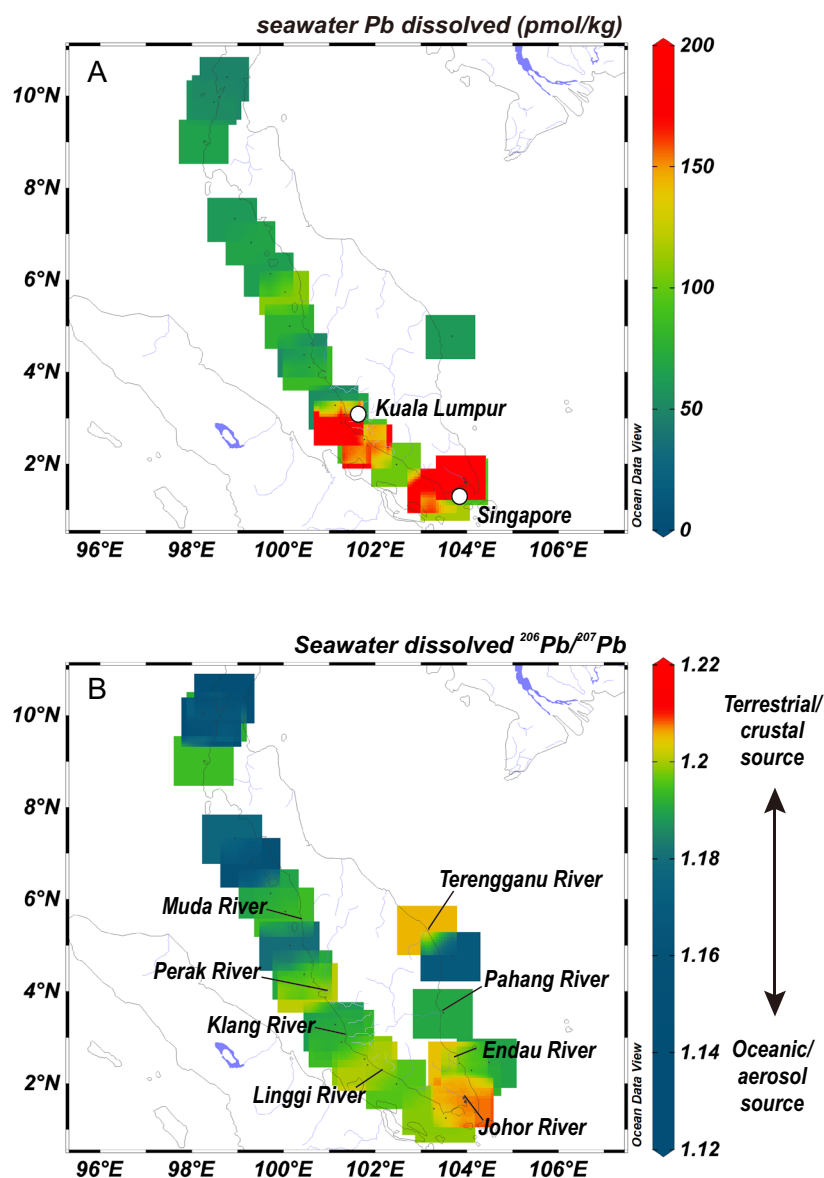


Fig. 2. Geographical distribution of (A) concentration and (B) isotopes of dissolved Pb in seawater samples around the Malayan Peninsula. Major cities or rivers are also highlighted. Figure plotted through Ocean Data View (30).

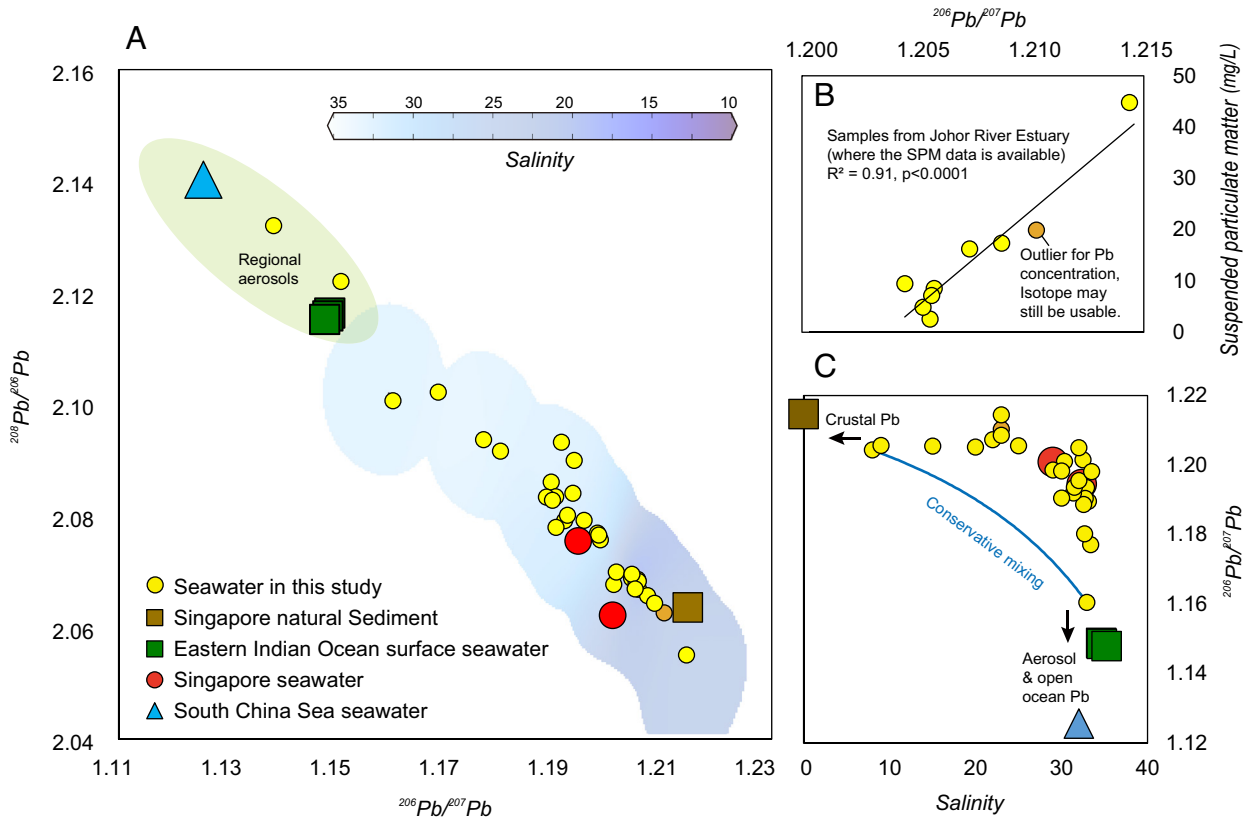


Fig. 3. Comparisons of Pb isotopes in seawater, salinity and SPM. (A) Triple-isotope plot of the seawater samples in this study in comparison with regional sources from three main references (28, 29, 31). The locations of the sites are the same as Fig. 1. The weighted-average salinity distribution was also indicated. (B) Scatter plot of the $^{206}\text{Pb}/^{207}\text{Pb}$ in Johor River estuary waters compared with SPM concentrations. Regression statistics are presented. (C) Scatter plot of dissolved $^{206}\text{Pb}/^{207}\text{Pb}$ ratios from this study (all samples) and identified endmembers against salinity. The calculated Pb isotope ratios based on conservative mixing between two endmembers (Johor River Stn 1, salinity = 8 pss; and Malacca Strait Stn 2, salinity = 33 pss) are plotted with a blue curve. The uncertainties for Pb isotope measurements are within the size of each symbol. The orange dot denotes a sample treated as an outlier for Pb concentration probably due to poor filtering, but its isotope ratios may still be usable as the dissolved and particulate pools are in equilibrium.

$^{206}\text{Pb}/^{207}\text{Pb}$ ratios at intermediate salinities indicating an exchange of dissolved and particulate Pb (Fig. 3C), which has been clearly identified in prior studies investigating the behavior of Pb in estuaries (20, 34). We propose that this exchange could produce higher $^{206}\text{Pb}/^{207}\text{Pb}$ values in seawater than those predicted by conservative mixing in the waters surrounding the Malayan Peninsula. This exchange process is supported by both the results from a closed-system Pb isotope exchange experiment (26) and the strong linear relationship between seawater Pb isotope ratios and suspended particulate matter (SPM) concentrations observed in this study ($R^2 = 0.91$, Fig. 3B).

Modeling Pb Transport from Estuary to the Adjacent Sea.

To explore the particulate-mediated transport of Pb across the salinity gradient, we developed a 1-D model based on the conservative mixing of the dissolved pool with addition of an exchangeable particulate pool (Fig. 4A and *SI Appendix, Text S1*). In the model analyses, we employed a commonly applied partition coefficient (K_d) to quantify the particulate-dissolved exchange. The model reproduced the observed distribution of Pb isotopes in the seawater adequately (brown line; Fig. 4A), with R^2 values (between modeled and observed ratios) of 0.67 for $^{206}\text{Pb}/^{207}\text{Pb}$, 0.62 for $^{208}\text{Pb}/^{206}\text{Pb}$, and 0.63 for $^{206}\text{Pb}/^{204}\text{Pb}$. However, the model fails to reproduce all the variability of Pb concentrations across the range of observed salinities (Fig. 4B). This inconsistency can be explained by additions of various proportions of anthropogenic Pb to the dissolved pool (Fig. 4), which is supported by the different geographical distributions of the Pb concentration and Pb isotopic composition around the Malayan Peninsula (Fig. 2A).

To test the effect on Pb isotopes when anthropogenic Pb is added as a source, we ran the K_d model with random additions of dissolved Pb having regional aerosol isotopic signatures (Fig. 4 and *SI Appendix, Text S1*). The simulation results show that in coastal waters (salinity $> \sim 30$ pss), even if the anthropogenic Pb contribution is enhanced, the re-equilibrated Pb isotopes will move parallel to the modeled curve with minimal deviation (Fig. 4). Further, when more anthropogenic Pb is added in the estuary (salinity ~ 20 pss), the resultant Pb isotope ratios in the model move in the opposite direction from the observation (Fig. 4), indicating that the observed scatter in Pb at mid-salinity sites may be caused by estuarine dynamics that are not captured by our parameterized model (34), or by addition of dissolved Pb with isotopic compositions dissimilar from aerosols, resulting in a small deviation (~ 0.01 for $^{206}\text{Pb}/^{207}\text{Pb}$) between observation and model. We conclude that particulate-dissolved exchange could overall reasonably explain the observed Pb isotopes around the Malayan Peninsula, and enrichment of anthropogenic Pb likely explains the various concentrations observed in the coastal areas of high salinity (Fig. 4).

Lastly, we compare the K_d model with a previous Pb reconstruction using corals from Singapore (*SI Appendix, Fig. S1 and Text S2*) (35). Corals directly precipitate their skeletons from seawater, and therefore, the Pb isotope in coral skeletons reflects the seawater dissolved pool (36). The model does not reproduce the observed interannual variability (model-coral deviation around 0.01 to 0.02 for $^{206}\text{Pb}/^{207}\text{Pb}$), likely because our

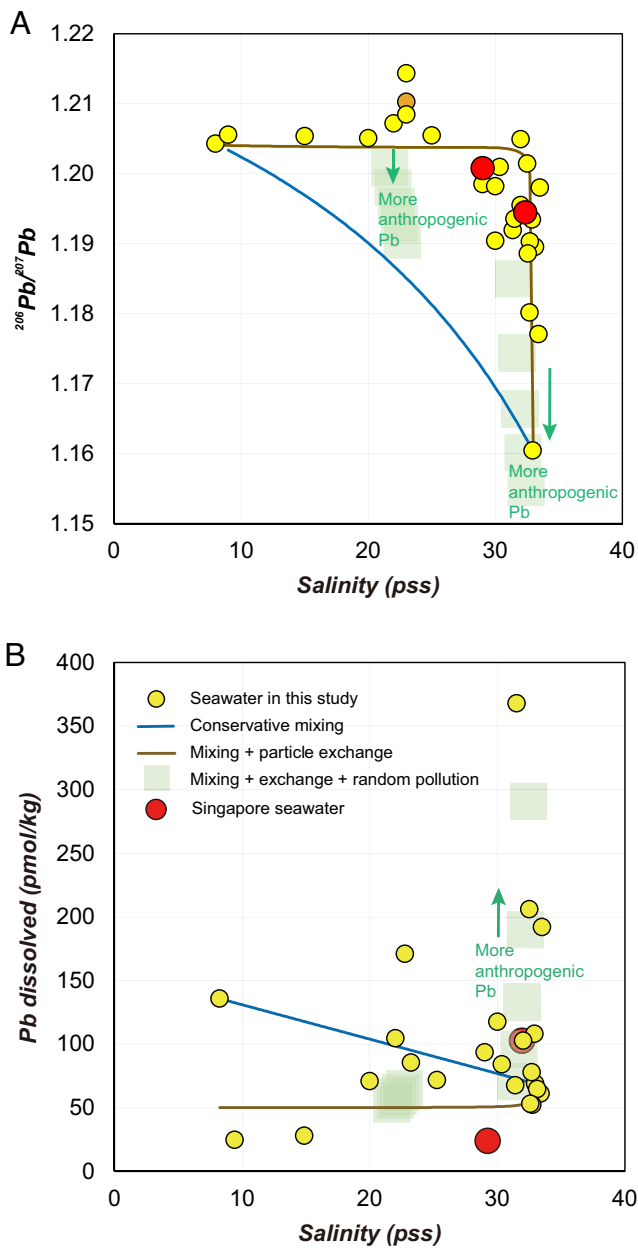


Fig. 4. Observation and modelling of (A) $^{206}\text{Pb}/^{207}\text{Pb}$ ratios and (B) concentrations of dissolved Pb compared with salinity. The locations of the sample sites are the same as Fig. 1. The conservative mixing model (blue line), the mixing plus particulate-dissolved exchange model (brown line), and the sensitivity test with random anthropogenic Pb additions (with Pb isotopic composition similar to regional aerosol) are also indicated in green squares. Uncertainties for Pb isotope measurements are within the size of the symbols.

parameterization is based on the large-scale salinity gradient and under-represents urbanized coastal areas (*SI Appendix, Text S2*). However, the K_d model largely explains the difference of Pb isotopes between the coral record and regional aerosols sources of Pb (coral-aerosol deviation ~ 0.06 , aerosol ~ 1.12 to 1.15 , coral ~ 1.18 to 1.20 for $^{206}\text{Pb}/^{207}\text{Pb}$, *SI Appendix, Fig. S1*), further supporting the case of substantial particulate-dissolved exchange in coastal waters.

Discussion

Although our field study does not cover a large expanse of the global coastal ocean, our findings are consistent with studies conducted worldwide. Exchange between dissolved and particulate

pools has been reported for several continental margins where sedimentary Pb inputs with crustal-like isotopic compositions were observed, including the western Philippine Sea (23), the Celtic Sea (24), and the Eastern Atlantic margin (25). In the northern Indian Ocean, the seawater $^{206}\text{Pb}/^{207}\text{Pb}$ signature from the Bay of Bengal was 0.005 to 0.010 higher than that from the Arabian Sea, while the Pb concentrations of the two regions were almost identical (28). The isotopic difference is not likely explained by differences in anthropogenic sources, as the offset is observed throughout the water column, whereas the anthropogenic Pb in the northern Indian Ocean is largely confined to the upper waters (28). Therefore, the most likely explanation is that sediments derived from rivers, including the Ganges-Brahmaputra, Irrawaddy, and Salween River and numerous smaller rivers draining to the sea, modify the isotopic composition of dissolved Pb in the Bay of Bengal to align more with that of crustal sources (28).

Given the scattered evidence on particulate-dissolved exchange around the world, the importance of this process for the marine Pb cycling prompted us to investigate how much this process contributes to seawater chemistry in both the present-day and pre-Anthropocene oceans. Using the K_d model with a step increase in seawater Pb concentration from 0 to 100 pmol/kg, our simulations suggest that particles scavenge Pb when the dissolved pool exceeds ~ 25 pmol/kg. Conversely, particles release Pb to the dissolved pool at lower seawater Pb concentrations (*SI Appendix, Fig. S2A*). Here we stress that 25 pmol/kg is our specific model result, not a universal threshold. However, this simulation result lends credence to the supposition that the seawater dissolved Pb concentration, in part, modulates the net particulate-dissolved exchange flux of Pb to the ocean dynamically. Given the expected large variability of dissolved Pb concentrations in coastal seas, our model result is consistent with observations of the non-uniform behavior of Pb in estuaries around the world, including net removal from dissolved phases by particles (18, 34, 37), as well as both quasi-conservative transport with salinity gradient (18, 38, 39) and reversible (two-way) exchange between dissolved and particulate phases (34, 38).

Further, the Pb in the present-day ocean is overprinted by a large anthropogenic input (40), resulting in high Pb concentrations in the coastal waters (e.g., refs. 41 and 42). Therefore, in today's ocean, fluvial particles are usually net sinks of Pb, with isotope exchange occurring between the dissolved and particulate pools (Fig. 5). Observations from outside the Amazon River mouth (with salinities 32 to 35 pss) are consistent with this hypothesis. The $^{206}\text{Pb}/^{207}\text{Pb}$ in the tropical Atlantic waters influenced by Amazon river plume are approximately 1.17 to 1.18, suggesting a significant contribution of crustal origin (43). The Pb concentrations in these waters (~ 15 to 18 pmol/kg) were lower than other places in the Western tropical Atlantic (~ 20 to 24 pmol/kg). The lowered Pb concentration associated with reworked isotopic composition in the Amazon-influenced seawater agree well with what our model predicts for particulate-dissolved exchange.

Conversely, we would expect lower dissolved Pb concentrations in seawater prior to the Anthropocene, whereby desorption from terrestrial particles was likely a more important source of Pb to seawater. The average Pb concentration in the pre-Anthropocene ocean has been estimated at ~ 2 pmol/kg (12), and the Pb concentration in the coastal water can be several folds higher: e.g., estimated to be about 10 pmol/kg from coral records in Bermuda (36) and Sumatra (29). If an average 6 pmol/kg of Pb is assumed, we estimate the fluvial particle exchange flux in the pre-Anthropocene ocean was on the order of $\sim 2.93 \times 10^7$ mol/y (range 2.31×10^7 to 3.56×10^7 mol/y, based on the Pb concentration in seawater of

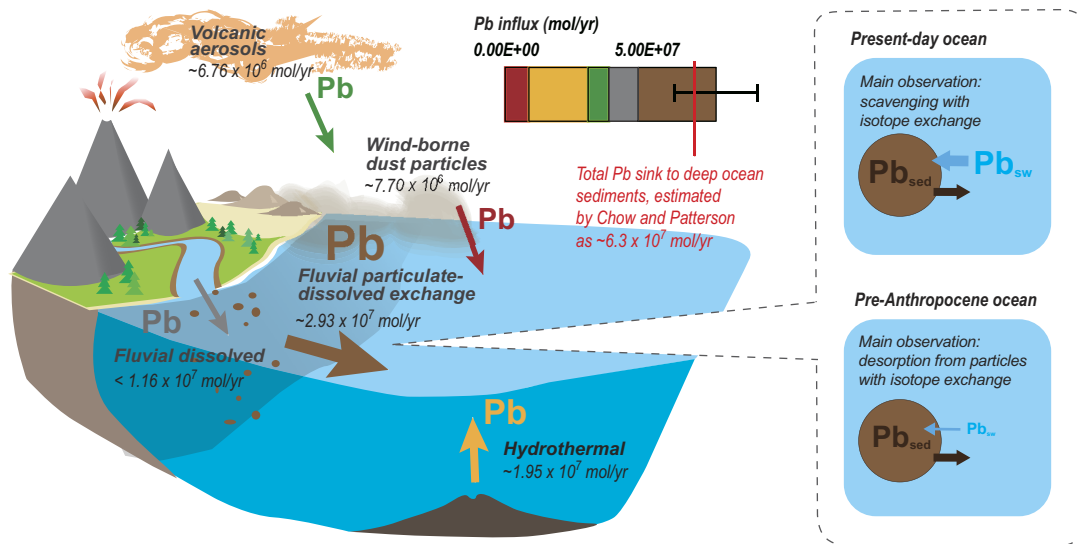


Fig. 5. Conceptual illustration of the estimate Pb flux from natural sources in the pre-Anthropocene ocean. In addition to fluvial particulates (this study), estimates of other natural sources include wind-borne dust particles (12), volcanic aerosols (11), hydrothermal systems (13, 14), and fluvial dissolved inputs (15), are also illustrated. The two *Inset* figures on the right illustrate the expected behavior and observation of particulate-dissolved Pb exchange in the present-day and pre-Anthropocene ocean.

2 to 10 pmol/kg; *SI Appendix, Fig. S2B*), which is about 30 to 40% of the global Pb flux to the ocean (Fig. 5 and *SI Appendix, Fig. S2B*). This estimated flux assumes similar geophysical conditions as those in the present day [e.g., weathering intensity, rainfall-runoff regime, fluvial SPM flux (44)].

To test the sensitivity of this estimated flux, we varied the particulate exchangeable pool ($\pm 50\%$), which is a significant amplitude, given relatively stable global weathering fluxes on different geological time scales (45–47). This variation resulted in an estimated flux range of 1.51×10^7 to 4.40×10^7 mol/y. The lower bound of this simulated fluvial particulate-dissolved exchange flux is comparable with other major Pb sources to the ocean (Fig. 5 and *SI Appendix, Fig. S2B*), suggesting that crustal particles discharged at continental margins are a major source of Pb to the pre-Anthropocene ocean. Our estimation compares well with the budget proposed by Chow and Patterson (10) that estimated a significant pre-anthropogenic fluvial Pb source entering the ocean (Fig. 5). Our study builds on this seminal work by identifying a plausible mechanism through which terrestrially derived materials influence the distribution of Pb in the ocean beyond fluvial plumes. Improved understanding of this mechanism involving particulate-dissolved Pb exchange should also aid in interpreting climate-modulated weathering signals in sedimentary records (e.g., ref. 48).

The influence of particulate-dissolved Pb exchange is also traceable in the pre-Anthropocene deep ocean, as revealed by a compilation of seawater Pb isotope reconstructions based on ferromanganese crusts and authigenic sediment coatings (*SI Appendix, Fig. S3*). Boundary exchange in the western North Atlantic, which has been shown to be a major factor determining deep ocean Neodymium isotopic composition (49), also likely influences Pb isotopic composition in this region. In particular, incongruent weathering plays an important role in releasing more radiogenic Pb isotopes from ice sheet-denuded materials along the continental margin (50) (*SI Appendix, Fig. S3*). North Atlantic Deep Water (NADW) carries the radiogenic isotope signal southward, with only some fraction reaching the Southern Ocean because of the relatively short residence time of Pb in the ocean [a couple of hundred years (51)]. Imprinted on some

terrestrial-derived detritus sourced from the East Antarctica, the radiogenic Pb signature of NADW can still be seen in the Indian Ocean sector of the Southern Ocean due to the transport of Circumpolar Deep Water (52, 53) (*SI Appendix, Fig. S3*). Another deep ocean region with potentially significant boundary Pb exchange is the northeastern Indian Ocean, where more radiogenic Pb is registered than in other Indian Ocean domains (53, 54) (*SI Appendix, Fig. S3*). The most parsimonious explanation for the isotope anomaly in this region is the exchange of Pb isotopes between seawater and the terrestrial sediments discharged from the Trans-Himalayan complex to the Bengal Fan, which is also consistent with seawater results discussed above (28).

Finally, in addition to providing evidence of the importance of boundary exchange in marine Pb cycling, our study provides reference points for investigating the boundary exchange of other elements. The importance of terrestrial particulate materials in marine element cycles has received increasing attention, but so far systematic studies have been mainly focused on a few elements (1). Considering that river discharge of particulate matter dominates the total flux of most elements to the global ocean (8), future studies on the exchange between particulate and dissolved phases are vital for understanding the processes driving element and isotope distributions in modern oceans (e.g., refs. 55 and 56), as well as weathering and climate feedback in the past revealed by proxy records (e.g., refs. 47 and 57).

Materials and Methods

Site and Sampling. Four cruises were conducted around the Malayan Peninsula (equatorial Southeast Asia) between 2016 and 2017 (*SI Appendix, Table S1*), including those focused on the Andaman coast near Ranong (Thailand), the Malacca Strait (Malaysia, Singapore), the Eastern Malaya Peninsula Coast (Malaysia), and the Johor River estuary (Malaysia). The Malacca Strait is a shallow (average depth ~ 27 m) channel in the tropical Southeast Asia, connecting the southern South China Sea and the Eastern Indian Ocean (Fig. 1). The current in Malacca Straits reverses seasonally in response to the monsoon—overall northwestward in northern hemisphere winter and southeastward in summer (58). Terrestrial material enters the strait from numerous rivers on the Malayan Peninsula and Sumatra Island, both of which are on the Eurasian Plate (59) (Fig. 1B). The Pb isotopic composition of the crustal particulates shows $^{206}\text{Pb}/^{207}\text{Pb}$

ratios >1.2 and $^{206}\text{Pb}/^{204}\text{Pb}$ ratios of about 19, which correspond with both ore minerals and natural sediments (60–62). The crustal Pb isotope offsets from the regional aerosols with $^{206}\text{Pb}/^{207}\text{Pb} \sim 1.15$ (31, 32, 63), the latter are believed to be the main source of Pb to the ocean (64).

We sampled seawater at 34 locations by lowering a polycarbonate pole into the water upstream of the boat. Sampling depth was within 1 m of the surface. A trace-metal-clean bottle was attached with the pole to collect the water sample. Upon collection, the seawater samples were filtered through a trace metal clean filter (0.4 μm pore size, Whatman Nuclepore™) within 24 h following trace metal protocols (65). Ancillary parameters including salinity and the concentration of SPM were measured during most cruises. The salinity was measured by a conductivity-temperature-depth (CTD) sensor on board (Seabird) or a refractometer when the CTD is not available. The accuracy of salinity was 0.01 pss for CTD and ~ 0.2 pss for refractometer. The SPM was measured by filtering 1 L of seawater through a pre-weighed GF/F filter and then frozen to -20°C on board. In the laboratory, the filters were oven-dried at 75°C for 24 h then mass determinations were made on a microbalance (66). Detailed information about the dates of the cruises and availability of ancillary data can be found in *SI Appendix, Table S1*.

Analytical Method on Seawater Pb Concentration and Isotopes. The preparation and analytical method for the determination of seawater Pb concentration and isotopes closely followed GEOTRACES protocols (65). The Pb concentration was measured using isotope dilution after single batch nitrilotriacetate (NTA) resin extraction (67). Briefly, each 1 mL of seawater sample was spiked with a ^{204}Pb -enriched solution of known concentration (Oak Ridge National Laboratory), an ammonium acetate buffer (pH = 5.3), and NTA resin beads (approximately 2,400 beads, cleaned) for Pb uptake. After 4 d of uptake, the beads were rinsed several times and eluted of Pb in 0.1 M of high-purity nitric acid (Optima grade, Thermo Fisher) for analysis on an Inductive Coupled Plasma Mass Spectrometer (ICP-MS) at Center for Environmental Sensing and Modeling (CENSAM), Singapore-MIT (Massachusetts Institute of Technology) Alliance on Research and Technology. The precision of the measurements was determined by independently preparing and running each sample in at least triplicates; and the concentration was accepted when at least two out of three replicates agreed. The accuracy of the measurements was determined by running the GEOTRACES SAFE D1 seawater, for which we determined a Pb concentration of 26.4 ± 1.4 pmol/kg ($n = 4$) which is not significantly different from the consensus value of 27.7 ± 2.6 pmol/kg (41, 68).

The Pb isotope composition of the seawater was measured using a multi-collector ICP-MS housed in the environmental geochemistry laboratory, Nanyang Technological University of Singapore, after an extraction of Pb through magnesium hydroxide ($\text{Mg}(\text{OH})_2$) co-precipitation and purification through hydrochloric-bromic acid (HCl-HBr) ion exchange chromatography (69). Briefly, 100 mL aliquots of seawater were added into two trace-metal-clean centrifuge tubes. A minimal amount of vapor-distilled ammonia solution was added to the seawater to trigger $\text{Mg}(\text{OH})_2$ precipitation that scavenged the Pb from the sample. The precipitate was redissolved in Optima grade HCl (Thermo Fisher), and the liquids

from the two centrifuge tubes were combined and precipitated again to further concentrate the Pb into a smaller amount of $\text{Mg}(\text{OH})_2$. The overall precipitate was then dissolved in a minimal amount of 1.1 M Optima grade HBr (ThermoFisher). Then loaded into Eichrom AG-1X8 anion exchange resin (chloride form, 200 to 400 mesh) columns and purified via HCl-HBr chromatography. The column blank was typically less than 7 pg, compared with the 1 to 2 ng of Pb in the seawater sample. The precision and accuracy of the Pb isotope analysis were compared with reference to replicates of standard reference material NBS981, which indicated high measurement quality even at low level of detection (typically 1 to 2 ng of Pb, *SI Appendix, Table S2*). In addition, we conducted an inter-laboratory comparison of the Pb isotope in seawater with Boyle's laboratory at MIT. The inter-laboratory comparison on the same sample shows highly comparable results (*SI Appendix, Table S2*). These comparisons suggest that our Pb isotope measurement should be good to ± 0.001 (2SD) for $^{206}\text{Pb}/^{207}\text{Pb}$ or better.

Modeling the Particulate-Dissolved Pb Exchange. Please see the *SI Appendix, Texts S1 and S2* for detailed information on the modeling of regional Pb isotope compositions and global particulate-dissolved Pb exchange fluxes.

Data, Materials, and Software Availability. All data in this study is included as *SI Appendix*.

ACKNOWLEDGMENTS. This research was funded by the Singapore National Research Foundation (NRF) through the Singapore-MIT Alliance for Research and Technology CENSAM to M.C., G.C., and E.A.B.; NRF Intra-CREATE Seed Collaboration grant NRF2021-ITS007-0003 to M.C.; NRF Marine Environmental Sensing Network to J.T.; Singapore Ministry of Education AcRF Tier1 grant RT 06/19 to M.C. and X.W.; and the Overseas Talent Recruitment Program of China to N.Z.. X.W. acknowledges the support of MOE2019-T2-1-174 (S) and NRF2017NRF-NSFC001-047 grants for the geochemistry laboratory. This is Earth Observatory of Singapore (EOS) contribution number 496. We thank Patrick Martin, Jiawei Feng, Caroline Chia, and the crew of S/Y Indigo V for field assistance. We thank Lu Xu for scientific illustration. Permits: We thank the National Park Board Singapore for allowing this research (NP/RP16-156-2a). We are grateful for the permissions to sample in Malaysian water [Johor: P.T.N.J 3/8/6; Marine Park: JTLM 630-7 Jld. 4(17); Port Dickson: Prk. M.L.S.04/32-2 Jld. 7(9)].

Author affiliations: ^aTropical Marine Science Institute, National University of Singapore 119227, Singapore; ^bEarth Observatory of Singapore, Nanyang Technological University, Singapore 639798, Singapore; ^cState Key Laboratory of Estuarine and Coastal Research and Institute of Eco-Chongming, East China Normal University, Shanghai 200241, China; ^dAsian School of the Environment, Nanyang Technological University, Singapore 639798, Singapore; ^eFaculty of Science and Marine Environment, Universiti Malaysia Terengganu, Kuala Nerus 210030, Malaysia; ^fCentre of Environmental Sustainability and Water Security, Research Institute for Sustainable Environment, Universiti Teknologi Malaysia, 81310 Johor Bahru, Malaysia; ^gSingapore Centre for Environmental Life Sciences Engineering, Nanyang Technological University, Singapore 637551, Singapore; ^hFaculty of Fisheries Technology and Aquatic Resources, Maejo University, Chiang Mai 50290, Thailand; ⁱAndaman Coastal Research Center for Development, Faculty of Fisheries, Kasetsart University, Ranong 85120, Thailand; and ^jDepartment of Earth, Atmospheric, and Planetary Sciences, Massachusetts Institute of Technology, Cambridge, MA 02139

1. C. Jeandel, E. H. Oelkers, The influence of terrigenous particulate material dissolution on ocean chemistry and global element cycles. *Chem. Geol.* **395**, 50–66 (2015).
2. J. Viers, B. Dupré, J. Gaillardet, Chemical composition of suspended sediments in World Rivers: New insights from a new database. *Sci. Total Environ.* **407**, 853–868 (2009).
3. R. A. Duce *et al.*, The atmospheric input of trace species to the world ocean. *Global Biogeochem. Cycles* **5**, 193–259 (1991).
4. K. W. Bruland, R. Middag, M. C. Lohan, "8.2—Controls of trace metals in Seawater" in *Treatise on Geochemistry*, H. D. Holland, K. K. Turekian, Eds. (Elsevier, Oxford, ed. 2, 2014), pp. 19–51, 10.1016/B978-0-08-095975-7.00602-1.
5. C. R. Pearce, M. T. Jones, E. H. Oelkers, C. Pradoux, C. Jeandel, The effect of particulate dissolution on the neodymium (Nd) isotope and Rare Earth Element (REE) composition of seawater. *Earth Planet. Sci. Lett.* **369–370**, 138–147 (2013).
6. P. J. Tréguier, C. L. D. L. Rocha, The World Ocean silica cycle. *Annu. Rev. Mar. Sci.* **5**, 477–501 (2013).
7. M. T. Jones *et al.*, Riverine particulate material dissolution as a significant flux of strontium to the oceans. *Earth Planet. Sci. Lett.* **355–356**, 51–59 (2012).
8. E. H. Oelkers *et al.*, The role of riverine particulate material on the global cycles of the elements. *Appl. Geochem.* **26**, S365–S369 (2011).
9. J. Gaillardet, B. Dupré, C. J. Allègre, Geochemistry of large river suspended sediments: Silicate weathering or recycling tracer? *Geochim. Cosmochim. Acta* **63**, 4037–4051 (1999).
10. T. J. Chow, C. Patterson, The occurrence and significance of lead isotopes in pelagic sediments. *Geochim. Cosmochim. Acta* **26**, 263–308 (1962).
11. C. C. Patterson, D. M. Settle, Review of data on eolian fluxes of industrial and natural lead to the lands and seas in remote regions on a global scale. *Mar. Chem.* **22**, 137–162 (1987).
12. G. M. Henderson, E. Maier-Reimer, Advection and removal of ^{210}Pb and stable Pb isotopes in the oceans: A general circulation model study. *Geochim. Cosmochim. Acta* **66**, 257–272 (2002).
13. J. C. Alt, Hydrothermal fluxes at mid-ocean ridges and on ridge flanks. *C. R. Geosci.* **335**, 853–864 (2003).
14. C. R. German, M. V. Angel, Hydrothermal fluxes of metals to the oceans: A comparison with anthropogenic discharge. *Geol. Soc. London Spec. Publ.* **87**, 365–372 (1995).
15. S. Jiang, Distribution and behavior of dissolved lead in the Antarctic Peninsula and the Northwestern Pacific Ocean, PhD thesis, East China Normal University, Shanghai, China (2021).
16. J. O. Nriagu, Global metal pollution: Poisoning the biosphere? *Environment* **32**, 7–33 (1990).
17. M. Baskaran, P. H. Santschi, The role of particles and colloids in the transport of radionuclides in coastal environments of Texas. *Mar. Chem.* **43**, 95–114 (1993).
18. H. Windom *et al.*, Trace metal transport in a tropical estuary. *Mar. Chem.* **24**, 293–305 (1988).
19. L. K. Benninger, ^{210}Pb balance in Long Island Sound. *Geochim. Cosmochim. Acta* **42**, 1165–1174 (1978).
20. F. Elbaz-Poulichet, P. Holliger, W. Wen Huang, J.-M. Martin, Lead cycling in estuaries, illustrated by the Gironde estuary, France. *Nature* **308**, 409–414 (1984).
21. C. Jeandel, Overview of the mechanisms that could explain the 'Boundary Exchange' at the land-ocean contact. *Philos. Trans. A Math. Phys. Eng. Sci.* **374**, 20150287 (2016).
22. L. Bridgestock *et al.*, Estuarine processes modify the isotope composition of dissolved riverine barium fluxes to the ocean. *Chem. Geol.* **579**, 120340 (2021).

23. C.-T. Chien, T.-Y. Ho, M. E. Sanborn, Q.-Z. Yin, A. Paytan, Lead concentrations and isotopic compositions in the Western Philippine Sea. *Mar. Chem.* **189**, 10–16 (2017).
24. D. Ruscicka *et al.*, Anthropogenic signatures of lead in the Northeast Atlantic. *Geophys. Res. Lett.* **45**, 2734–2743 (2018).
25. A. E. Noble *et al.*, Dynamic variability of dissolved Pb and Pb isotope composition from the U.S. North Atlantic GEOTRACES transect. *Deep Sea Res. Part II* **116**, 208–225 (2015).
26. M. Chen *et al.*, Lead isotope exchange between dissolved and fluvial particulate matter: A laboratory study from the Johor River estuary. *Philos. Trans. A Math. Phys. Eng. Sci.* **374**, 20160054 (2016).
27. J. D. Milliman, K. L. Farnsworth, *River Discharge to the Coastal Ocean: A Global Synthesis* (Cambridge University Press, 2011).
28. J.-M. Lee *et al.*, Impact of anthropogenic Pb and ocean circulation on the recent distribution of Pb isotopes in the Indian Ocean. *Geochim. Cosmochim. Acta* **170**, 126–144 (2015).
29. J.-M. Lee *et al.*, Coral-based history of lead and lead isotopes of the surface Indian Ocean since the mid-20th century. *Earth Planet. Sci. Lett.* **398**, 37–47 (2014).
30. R. Schlitzer, Ocean data view, <https://odv.awi.de/>, (2021). Accessed 1 May 2022.
31. G. Carrasco *et al.*, An update of the Pb isotope inventory in post leaded-petrol Singapore environments. *Environ. Pollut.* **233**, 925–932 (2018).
32. J. Kayee, S. Bureekul, P. Sompongchaiyakul, X. Wang, R. Das, Sources of atmospheric lead (Pb) after quarter century of phasing out of leaded gasoline in Bangkok, Thailand. *Atmos. Environ.* **253**, 118355 (2021).
33. R. Das, A. T. Bin Mohamed Mohtar, D. Rakshit, D. Shome, X. Wang, Sources of atmospheric lead (Pb) in and around an Indian megacity. *Atmos. Environ.* **193**, 57–65 (2018).
34. K.-T. Jiann, L.-S. Wen, P. H. Santschi, Trace metal (Cd, Cu, Ni and Pb) partitioning, affinities and removal in the Danshuei River estuary, a macro-tidal, temporally anoxic estuary in Taiwan. *Mar. Chem.* **96**, 293–313 (2005).
35. M. Chen, J.-M. Lee, I. S. Nurhati, A. D. Switzer, E. A. Boyle, Isotopic record of lead in Singapore straits during the last 50 years: Spatial and temporal variations. *Mar. Chem.* **168**, 49–59 (2015).
36. A. E. Kelly, M. K. Reuer, N. F. Goodkin, E. A. Boyle, Lead concentrations and isotopes in corals and water near Bermuda, 1780–2000. *Earth Planet. Sci. Lett.* **283**, 93–100 (2009).
37. A. R. Abdel-Moati, Behaviour and fluxes of copper and lead in the Nile River estuary. *Estuar. Coast. Shelf Sci.* **30**, 153–165 (1990).
38. F. ç. Elbaz-Poulichet, J.-M. Garnier, D. M. Guan, J.-M. Martin, A. J. Thomas, The conservative behaviour of trace metals (Cd, Cu, Ni and Pb) and As in the surface plume of stratified estuaries: Example of the Rhône River (France). *Estuar. Coast. Shelf Sci.* **42**, 289–310 (1996).
39. R. Cenci, J.-M. Martin, Concentration and fate of trace metals in Mekong River Delta. *Sci. Total Environ.* **332**, 167–182 (2004).
40. A. B. Boyle *et al.*, Anthropogenic lead emissions in the Ocean: The evolving global experiment. *Oceanography* **27**, 69–75 (2014).
41. S. Jiang, J. Zhang, R. Zhang, Y. Xue, W. Zheng, Dissolved lead in the East China Sea with implications for impacts of marginal seas on the open ocean through cross-shelf exchange. *J. Geophys. Res.: Oceans* **123**, 6004–6018 (2018).
42. M. Chen *et al.*, Monsoonal variations of lead (Pb) in coastal waters around Singapore. *Mar. Pollut. Bull.* **179**, 113654 (2022).
43. L. Bridgestock *et al.*, Return of naturally sourced Pb to Atlantic surface waters. *Nat. Commun.* **7**, 12921 (2016).
44. D. Walling, D. Fang, Recent trends in the suspended sediment loads of the world's rivers. *Global Planet. Change* **39**, 111–126 (2003).
45. G. L. Foster, D. Vance, Negligible glacial-interglacial variation in continental chemical weathering rates. *Nature* **444**, 918–921 (2006).
46. F. Von Blanckenburg, J. Bouchez, D. E. Ibarra, K. Maher, Stable runoff and weathering fluxes into the oceans over quaternary climate cycles. *Nat. Geosci.* **8**, 538–542 (2015).
47. J. K. Caves Rugenstein, D. E. Ibarra, F. von Blanckenburg, Neogene cooling driven by land surface reactivity rather than increased weathering fluxes. *Nature* **571**, 99–102 (2019).
48. D. J. Wilson, A. Galy, A. M. Piotrowski, V. K. Banakar, Quaternary climate modulation of Pb isotopes in the deep Indian Ocean linked to the Himalayan chemical weathering. *Earth Planet. Sci. Lett.* **424**, 256–268 (2015).
49. F. Lacan, C. Jeandel, Neodymium isotopes as a new tool for quantifying exchange fluxes at the continent–ocean interface. *Earth Planet. Sci. Lett.* **232**, 245–257 (2005).
50. F. von Blanckenburg, T. F. Nägler, Weathering versus circulation-controlled changes in radiogenic isotope tracer composition of the Labrador Sea and North Atlantic deep water. *Paleoceanography* **16**, 424–434 (2001).
51. M. Frank, Radiogenic isotopes: Tracers of past ocean circulation and erosional input. *Rev. Geophys.* **40**, 1–1–1–38 (2002).
52. W. Abouchami, S. L. Goldstein, A lead isotopic study of circum-antarctic manganese nodules. *Geochim. Cosmochim. Acta* **59**, 1809–1820 (1995).
53. I. Vlastélic, W. Abouchami, S. Galer, A. Hofmann, Geographic control on Pb isotope distribution and sources in Indian Ocean Fe–Mn deposits. *Geochim. Cosmochim. Acta* **65**, 4303–4319 (2001).
54. M. Frank, R. O'Nions, Sources of Pb for Indian Ocean ferromanganese crusts: A record of Himalayan erosion? *Earth Planet. Sci. Lett.* **158**, 121–130 (1998).
55. S. G. John, J. Mendez, J. Moffett, J. Adkins, The flux of iron and iron isotopes from San Pedro Basin sediments. *Geochim. Cosmochim. Acta* **93**, 14–29 (2012).
56. M. Lambelet *et al.*, Neodymium isotopic composition and concentration in the western North Atlantic Ocean: Results from the GEOTRACES GA02 section. *Geochim. Cosmochim. Acta* **177**, 1–29 (2016).
57. E. T. Tipper *et al.*, Global silicate weathering flux overestimated because of sediment–water cation exchange. *Proc. Natl. Acad. Sci. U.S.A.* **118**, e2016430118 (2021).
58. B. Mayer, T. Stacke, I. Stottmeister, T. Pohlmann, Sunda shelf seas: Flushing rates and residence times. *Ocean Sci. Discuss.* **12**, 863–895 (2015).
59. A. J. Barber, M. J. Crow, Structure of Sumatra and its implications for the tectonic assembly of Southeast Asia and the destruction of Paleotethys. *Isl. Arc* **18**, 3–20 (2009).
60. C. Makouidi *et al.*, Geology, geochemistry and metallogenesis of the Selinsing gold deposit, central Malaysia. *Gondwana Res.* **26**, 241–261 (2014).
61. M. Gasparon, R. Varne, Crustal assimilation versus subducted sediment input in west Sunda arc volcanics: An evaluation. *Mineral. Petrol.* **64**, 89–117 (1998).
62. M. Chen, E. A. Boyle, A. D. Switzer, C. Gouramanis, A century long sedimentary record of anthropogenic lead (Pb), Pb isotopes and other trace metals in Singapore. *Environ. Pollut.* **213**, 446–459 (2016).
63. A. Bollhöfer, K. J. R. Rosman, Isotopic source signatures for atmospheric lead: The Southern Hemisphere. *Geochim. Cosmochim. Acta* **64**, 3251–3262 (2000).
64. A. R. Flegal, Lead in tropical marine systems: A review. *Sci. Total Environ.* **58**, 1–8 (1986).
65. G. A. Cutter *et al.*, Sampling and Sample-Handling Protocols for GEOTRACES Cruises (Version 3), GEOTRACES International Project Office, Toulouse, France. (2017).
66. Y. Liang *et al.*, Assessment of physical-chemical water quality characteristics and heavy metals content of lower Johor River, Malaysia. *J. Environ. Treat. Tech.* **8**, 961–966 (2020).
67. J.-M. Lee *et al.*, Analysis of trace metals (Cu, Cd, Pb, and Fe) in seawater using single batch nitrotriacetate resin extraction and isotope dilution inductively coupled plasma mass spectrometry. *Anal. Chim. Acta* **686**, 93–101 (2011).
68. GEOTRACES, Standards and reference materials. Retrieved (2022). <https://www.geotraces.org/standards-and-reference-materials/> (n.d.).
69. E. A. Boyle *et al.*, GEOTRACES IC1 (BATS) contamination-prone trace element isotopes Cd, Fe, Pb, Zn, Cu, and Mo intercalibration. *Limnol. Oceanogr.: Methods* **10**, 653–665 (2012).